Estimation of the Activation Energy in the Belousov−Zhabotinsky Reaction by Temperature Effect on Excitable Waves

Jinzhong Zhang,[†] Luqun Zhou,[†] and Qi Ouyang*[,†,‡,§]

Department of Physics, The Beijing−Hong Kong−Singapore Joint Center for Nonlinear and Complex Systems (PKU), and Center for Theoretical Biology, Peking University, Beijing 100871, People's Republic of China

Received: October 7, 2006; In Final Form: November 26, 2006

We report the temperature effect on the propagation of excitable traveling waves in a quasi-two-dimensional Belousov−Zhabotinsky reaction−diffusion system. The onset of excitable waves as a function of the sulfuric acid concentration and temperature is identified, on which the sulfuric acid concentration exhibits an Arrhenius dependence on temperature. On the basis of this experimental data, the activation energy of the self-catalyzed reaction in the Oregonator model is estimated to be 83−113 kJ/mol, which is further supported by our numerical simulations. The estimation proceeds without analyzing detailed reaction steps but rather through observing the global dynamic behaviors in the BZ reaction. For a supplement, the wave propagation velocities are calculated based on our results and compared with the experimental observations.

Introduction

The Belousov−Zhabotinsky (BZ) reaction has been studied for decades.[1,2] It is often considered to be a simple experimental model to demonstrate nonlinear phenomena discussed in theories and compare with biological behaviors observed in living systems.[3,4] Different kinetic models have been developed to describe the reaction mechanism of the BZ reaction. Among them, the Oregonator[5] is the simplest model derived from the more completely discussed mechanism of Field−Körös−Noyes (FKN) kinetics.[6] It grasps the essential behaviors of the reaction and qualitatively agrees with most of the experimental observations.

The activation energies, which reflect the relationship between chemical reactions and temperature, are often investigated as elemental experimental parameters. Three of the five activation energies in the Oregonator model have been estimated by discussing the detail steps;[7,8] one of them is proved to be similar to the overall activation energy.[9] Here we concentrate on estimating the last activation energy that has still not been obtained.

Previously, two ways to estimate the activation energies in the BZ reactions are documented. One is to estimate the rates of an elementary reaction in different temperatures, as reported by Field[7,8] and Thompson;[10] the other is to observe the oscillation periods, which is most used to estimate the overall activation energy of the BZ reaction.[11−16] In this work, we use the information from the wave properties of the BZ reaction to estimate the activation energy.

The outline of this work is as follows: We first study the wave propagation behaviors in different temperatures, focusing on identifying the onset of excitable waves in the control parameter space. An Arrhenius dependence of sulfuric acid concentration on temperature can be obtained on the subexcitable−excitable boundary. Then, in order to relate this behavior to the realistic picture of the BZ reaction, we build the relation between the excitability of waves and parameter values in the Oregonator model using Karma's theory.[17] Taking the Arrhenius form to represent the temperature dependence of rate constants in the Oregonator, the range of the activation energy of the self-catalyzed reaction in the Oregonator model can be estimated. Finally, based on the estimated activation energy, we compare the expected and measured velocities of wave propagation in different temperatures.

Experimental Setup

Our spatial open reactor is similar to the equipment described previously.[18] In order to guarantee the necessary reaction diffusion feature of the system, a porous glass disk (Vycor glass 7390, Corning) is used as the reaction medium to prevent any convection motion. The disk is 0.4 mm in thickness and 25 mm in diameter with an average pore size of 10 nm. The opposite two sides of the porous glass disk are respectively in contact with two reactant reservoirs (10 mL in volume for each). The reactants are continuously pumped into the reservoirs by a highly precise tubing peristaltic pump (ISMATEC, IPC78001-10), whose flow rate is fixed at 36 mL/h for each reservoir. One reservoir is kept in the reduced state, consisting of [KBr] = 20 mM, [$NaBrO_3$] = 0.2 M, and [$CH_2(COOH)_2$] = 0.4 M. The other reservoir is kept in the oxidized state, consisting of [Ferroin] = 0.6 mM, [$NaBrO_3$] = 0.2 M, and H_2SO_4; its concentration is chosen as one of the control parameters. The reactants in both reservoirs are kept homogeneous by magnetic stirring. When the reactants diffuse from the two reservoirs to the reaction medium and meet together, the Ferroin-catalyzed BZ reactions occur, resulting in different sustained spatiotemporal patterns. In order to excite target waves in a certain direction, part of the glass on the side of the reduced state is covered with silicone rubber, as shown in Figure 1.

The reaction temperature is another control parameter in our experiment. To control the reaction temperature, the reservoirs in the reaction system are surrounded with a jacket, which is connected to a thermostatic water circulation system. A platinic thermistor (Pt100) is set on one of the reservoirs near the porous glass but not in contact with the reactants. The thermistor feeds back signals to a PID temperature controller in the thermostatic water circulation system so that the reservoirs and the glass can be kept at an expected temperature within ±0.1 °C.

* To whom correspondence may be addressed. E-mail: qi@pku.edu.cn.
† Department of Physics.
‡ The Beijing−Hong Kong−Singapore Joint Center for Nonlinear and Complex Systems (PKU).
§ Center for Theoretical Biology.

10.1021/jp0665978 CCC: $37.00 © 2007 American Chemical Society
Published on Web 01/24/2007

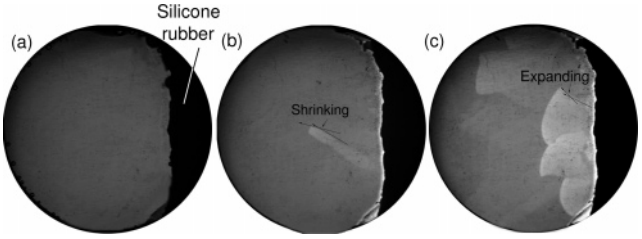

Figure 1. Photographs of our experimental states: (a) no wave appearing; (b) weakly excitable (subexcitable) state; (c) excitable state.

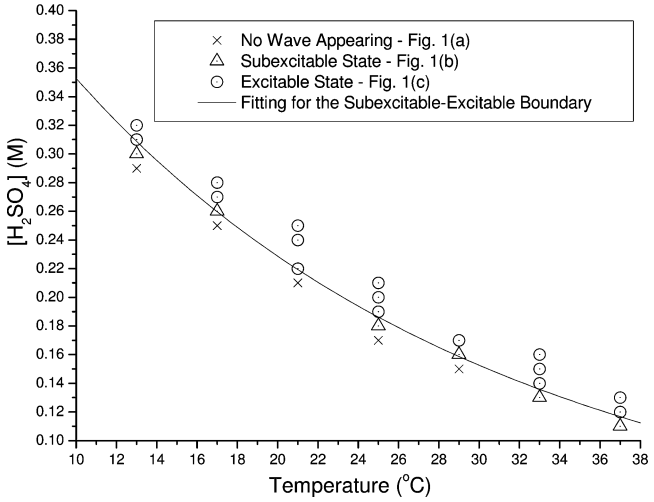

Figure 2. Phase diagram in the plane of ($[H_2SO_4]$, temperature) showing the onset of the excitable waves.

Experimental Results

For a fixed temperature, our experiment begins at a low $[H_2SO_4]$, such that no wave appears in the glass, as shown in Figure 1a. This is an unexcitable state. With increase in $[H_2SO_4]$, the region covered with silicone rubber begins to excite waves. However, the waves shrink and fade out while propagating, as shown in Figure 1b. We call this state a weakly excitable or subexcitable state.[19] With further increase in $[H_2SO_4]$, waves excited from the silicone rubber region can expand and coil while propagating, as shown in Figure 1c. The system is thus in an excitable state.

The boundaries between the subexcitable state and the excitable state depend on the reaction temperature. Figure 2 presents the phase diagram in the ($[H_2SO_4]$, temperature) plane. One observes that the onset of excitable waves decreases as the reaction temperature increases. We notice that the boundary in this plane can be fitted with an Arrhenius form:

$$[H_2SO_4]_c = \rho\cdot\exp\left(-\frac{\sigma}{RT_c}\right) (286\ \mathrm{K} \leqslant T_c \leqslant 310\ \mathrm{K}) \quad (1)$$

where $R = 8.31\ \mathrm{J\cdot mol^{-1}\cdot K^{-1}}$; $\rho = 1.2 \times 10^{-6}$ M; and $\sigma = -30$ kJ/mol. For simplicity, we consider only the first step of the sulfuric acid ionization; thus, eq 1 becomes $[H]_c(T_c) = [H]_{c_0} e^{-(\sigma/R)((1/T_c)-(1/T_{c0}))}$, where $H = H^+$. Setting T_{c_0} to 298 K, we get $[H]_{c_0} = 0.19$ M from eq 1 or the experimental data of Figure 2.

Theory and Simulation

In general, a two-variable reaction−diffusion model given by

$$\epsilon\frac{\partial u}{\partial t} = \epsilon^2\nabla^2 u + f(u,v)$$
$$\frac{\partial v}{\partial t} = \delta\epsilon\nabla^2 v + g(u,v) \qquad \epsilon \ll 1 \quad (2)$$

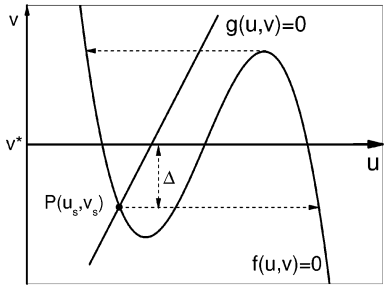

Figure 3. Typical phase plane for an excitable medium.[17]

TABLE 1: The Simplest Oregonator and Its Activation Energies

reactions	activation energies
$A + Y \xrightarrow{k_1} X + P$	$E_1 \approx 54$ kJ/mol[7]
$X + Y \xrightarrow{k_2} 2P$	$E_2 \approx 25$ kJ/mol[7]
$A + X \xrightarrow{k_3} 2X + Z$	E_3 (to be determined)
$X + X \xrightarrow{k_4{}^a} A + P$	$E_{4.1} \approx 23$ kJ/mol $E_{4.2} \approx 18$ kJ/mol[a,8]
$B + Z \xrightarrow{k_5} fY$	$E_5 \approx 70$ kJ/mol[9,11−15]

[a] The results of ref 8 show that k_4 should be represented as $k_{4.1} + k_{4.2}[H]$. $E_{4.1}$ is the activation energy for $k_{4.1}$ while $E_{4.2}$ is that for $k_{4.2}$ (in H_2SO_4 medium).

is useful to describe an excitable system. Its dynamics can be described by Figure 3. The system has only one fixed point (u_s,v_s). The excitability of the system can be measured by the parameter $\Delta = v^* - v_s$, where v^* is defined by the propagation velocity $c(v^*) = 0$.[20] Under the conditions of small ϵ and $\delta \approx 0$, the critical value Δ_c where the traveling wave will neither expend nor shrink is given by

$$\Delta_c = (g^*\epsilon/0.535\alpha^2)^{1/3} \quad (3)$$

where $\alpha \equiv (\mathrm{d}c(v_0))/(\mathrm{d}v_0)|_{v_0=v^*}$; $g^* \equiv g[h_+(v^*), v^*]$; $u = h_+(v)$ is the rightmost branch of the u nullcline $f(u,v) = 0$.[17] Δ_c determines the subexcitable−excitable boundary of the system.

We use the Oregonator model[5] to describe the excitable wave propagation in the experimental system. The kinetic equations and their activation energies are given in Table 1, where $A = BrO_3^-$; B stands for all organic substrates; $X = HBrO_2$; $Y = Br^-$; Z = 2·Ferroin; P = HOBr;[1] and k_i are the rate constants. The instantaneous reaction rates $v_1 = k_1[H]^2[A][Y]$,[1] $v_2 = k_2[H][X][Y]$,[1] $v_3 = k_3[H][A][X]$,[1] $v_4 = (k_{4.1} + k_{4.2}[H])[X]^2$,[8] $v_5 = k_5[B][Z]$.[1] For simplicity, except for k_4, k_i ($i = 1, 2, 3, 4.1, 4.2, 5$) is written as an Arrhenius form with a temperature-independent pre-exponential factor A_i: $k_i = A_i \exp(-E_i/RT) = k_{i0} \exp[-(E_i/R)((1/T) - (1/T_0))]$, where $k_{i0} = A_i \exp(-E_i/RT_0)$.

Considering [Y] is a fast variable that can be adiabatically eliminated,[20,21] the dimensionless form of the two-variable Oregonator model can be mapped to eq 2. The corresponding functions and variables are

$$f(u,v) = u - u^2 - fv\frac{u-q}{u+q}$$
$$g(u,v) = u - v$$
$$\delta = D_v/D_u$$
$$\epsilon = \frac{k_5[B]}{k_3[H][A]}$$

where

$$u = \frac{2k_4[X]}{k_3[H][A]};\ v = \frac{k_4k_5[B][Z]}{(k_3[H][A])^2};\ q = \frac{2k_1k_4}{k_2k_3};$$

D_u and D_v are respectively the diffusion coefficients of $HBrO_2$ and Ferroin; and f is a positive stoichiometric coefficient that cannot exceed 4 for chemical reasons.[1,22] Recent experiments revealed that f depends on temperature and $[H_2SO_4]$.[23−28] Our experiments are conducted in an excitable regime, so that $1 + \sqrt{2} \leqslant f \leqslant 4$.[22]

In order to obtain the parameters in eq 3, the propagation velocity of an isolated traveling excitable wave front must be calculated. According to Tyson,[21] it is given by

$$c(f,q,v_0) = [\int_{h\_(v_0)}^{h_+(v_0)} f(u,v_0)\mathrm{d}u]/L$$

$$L = \int_{-\infty}^{+\infty} \left(\frac{\mathrm{d}u}{\mathrm{d}\xi}\right)^2 \mathrm{d}\xi$$

where $\xi = [(k_5[B]/\sqrt{k_3[H][A]D_u})x - ct]/\epsilon$ (x is the coordinate of the wave propagation direction in real space, t is real time) and $h\_(v)$ is the leftmost branch of the u nullcline. L depends on the change rate of $[HBrO_2]$ in the wave propagation direction, which is controlled by the apparent wave amplitude in that direction. Because the amplitude does not change as a function of temperature in our experiments, we consider L to be independent of temperature. The order of magnitude of L can be estimated in the Oregonator model: As $u_s \approx 0$, $u_{max} \approx 0.5$ (which depends on q but changes slightly), the width of the wave front bounder where $\mathrm{d}u/\mathrm{d}\xi \neq 0$ is O(1), so $L \approx 10^{-1}$.

Following Tyson's calculation,[21] $h\_(v_0) \approx q$ and $h_+(v_0) \approx 1 - 2fv_0$, we have

$$c(f,q,v_0) = \frac{1}{6L}\{(1+q)^2(1-2q) - 6f(1+q)v_0 + 16f^3{v_0}^3 + 12fqv_0 \ln[2q(1+q-2fv_0)]\} \quad (4)$$

We use Newton's iteration starting from $v_0 = 0.05$ for two times (steps ① and ②) to obtain the analytic expression of $v^*(f,q)$:

$$① \begin{cases} \alpha_1(f,q) = \left.\dfrac{\partial c(f,q,v_0)}{\partial v_0}\right|_{v_0=0.05} \\ v_1^*(f,q) = 0.05 - \dfrac{c(f,q,0.05)}{\alpha_1} \end{cases}$$

$$② \begin{cases} \alpha(f,q) = \left.\dfrac{\partial c(f,q,v_0)}{\partial v_0}\right|_{v_0=v_1^*} \\ v^*(f,q) = v_1^* - \dfrac{c(f,q,v_1^*)}{\alpha} \end{cases}$$

Then we have the parameters in eq 3:

$$g^*(f,q) = h_+(v^*) - v^* = 1 - 2fv^* - v^*$$

$$\Delta(f,q) = v^* - v_s$$

$$\left[v_s(f,q) = \frac{1-q-f+\sqrt{(1-q-f)^2+4q(1+f)}}{2}\right]$$

Taking the calculated functions into eq 3, we obtain the critical ϵ:

$$\epsilon_c(f,q) = \frac{\Theta(f,q)}{L^2}$$
$$\Theta(f,q) = \frac{0.535\alpha^2(f,q)\Delta^3(f,q)L^2}{g^*(f,q)} \quad (5)$$

where $\Theta(f,q)$ is independent of L. These analytical results are in quantitative agreement with numerical simulations, as shown in Figure 4.

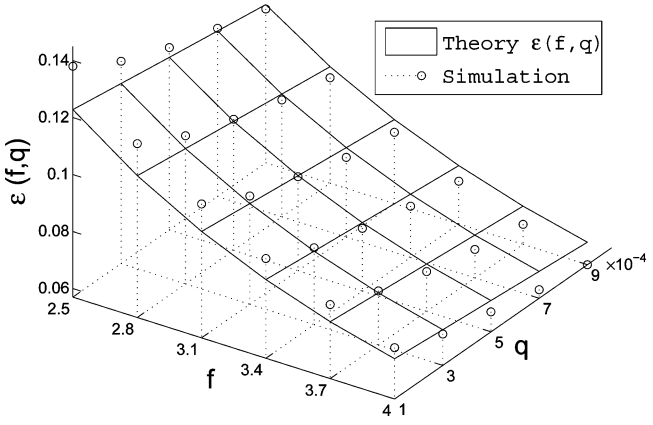

Figure 4. The analytical results of $\epsilon(f,q)$ compared with the numerical simulations. The excitable region is below the surface. $L = 0.10$ is in analytical form. In the numerical simulations, we search for an appropriate ϵ for each (f,q) following Showalter's criterion.[19] The parameters for the simulations are $\delta = 0.6$,[22] the grid is 400 × 100 points, the grid mesh is 0.15, and the time step is 0.001.

Now we take account of the temperature effect. $\epsilon = (k_5[B])/(k_3[H][A])$ in the Oregonator model, so that, at the onset of subexcitable−excitable transitions, we have

$$\epsilon_c(T_c) = \epsilon_{c_0}\frac{[H]_{c_0}}{[H]_c(T_c)} e^{-[(E_5-E_3)/R][(1/T_c)-(1/T_{c0})]} \quad (6)$$

where ϵ_{c_0} is the value of ϵ_c on T_{c_0}. At the onset of excitable waves, q_c changes as follows:

$$q_c(T_c) = q_{c_0}\cdot e^{-[(E_1-E_2+E_{4.1}-E_3)/R][(1/T_c)-(1/T_{c0})]} \cdot \frac{1+(k_{4.2_0}/k_{4.1_0})[H]_c e^{-[(E_{4.2}-E_{4.1})/R][(1/T_c)-(1/T_{c0})]}}{1+(k_{4.2_0}/k_{4.1_0})[H]_{c_0}} \quad (7)$$

where q_{c_0} is the value of q_c on T_{c_0} and $k_{4.2_0}/k_{4.1_0} = 1013/781 \approx 1.3$.[8] We define f_c as the value of f at the onset of excitable waves and f_{c_0} as the value of f_c on T_{c_0}. f_c is a function of T_c and should also satisfy $1 + \sqrt{2} \leqslant f_c \leqslant 4$. Combining eqs 5, 6, and 7, $[H]_c$ on the subexcitable−excitable boundary can be obtained:

$$[H]_c(T_c) = \frac{\Theta(f_{c_0},q_{c_0})}{\Theta[f_c, q_c(T_c)]}[H]_{c_0} e^{-[(E_5-E_3)/R][(1/T_c)-(1/T_{c0})]} \quad (8)$$

As shown in Figure 4, in the range of interest, $\Theta(f_c,q_c)$ is a monotonous decreasing function of f_c. So $[H]_c$ is a monotonous increasing function of f_c. As a result, defining $\Xi(T_c) = \Theta(f_{c_0},q_{c_0})[H]_{c_0}e^{-[(E_5-E_3)/R][(1/T_c)-(1/T_{c0})]}$, the following inequality can be obtained:

$$\frac{\Xi(T_c)}{\Theta[1+\sqrt{2}, q_c(T_c)]} \leqslant [H]_c(T_c) \leqslant \frac{\Xi(T_c)}{\Theta[4, q_c(T_c)]}$$

where 286 K $\leqslant T_c \leqslant$ 310 K.

After simplifying the inequality we get

$$-\ln\{\Theta[1+\sqrt{2}, q_c(T_c)]\} - \frac{E_5-E_3}{R}\left(\frac{1}{T_c} - \frac{1}{T_{c_0}}\right)$$

$$\leqslant -\ln[\Theta(f_{c_0}, q_{c_0})] - \frac{\sigma}{R}\left(\frac{1}{T_c} - \frac{1}{T_{c_0}}\right)$$

$$\leqslant -\ln\{\Theta[4, q_c(T_c)]\} - \frac{E_5 - E_3}{R}\left(\frac{1}{T_c} - \frac{1}{T_{c_0}}\right) \qquad (9)$$

where 286 K $\leqslant T_c \leqslant$ 310 K.

To estimate the quantity of E_3, we take the Taylor series of $\ln\{\Theta[f_c, q_c(1/T_c)]\}$ as a function of $1/T_c$ and evaluate it at $1/T_{c_0}$. We notice that, under our experimental conditions, $1 + \sqrt{2} \leqslant f_c \leqslant 4$, $0 < q_{c_0} \leq 10^{-3}$,[1,22] and 286 K $\leqslant T_c \leqslant$ 310 K. In addition, we know that E_3 is bigger than 50 kJ/mol and should not be very high as a result of the temperature effect on the excitable wave speeds (see the next section). Under these conditions, the orders higher than the first order in the Taylor series can be ignored. At room temperature, $q_{c_0} = 0.0002$,[1,22] so we get

$$\ln\{\Theta[1 + \sqrt{2}, q_c(T_c)]\} \approx -6.626 + \frac{(1.0\ \text{kJ/mol} - 0.022E_3)}{R}\left(\frac{1}{T_c} - \frac{1}{T_{c_0}}\right)$$

$$\ln\{\Theta[4, q_c(T_c)]\} \approx -7.216 + \frac{(1.0\ \text{kJ/mol} - 0.022E_3)}{R}\left(\frac{1}{T_c} - \frac{1}{T_{c_0}}\right) \qquad (10)$$

Our experimental result gives $\sigma = -30$ kJ/mol in inequation 9 (see the Experimental Results section). In this case, the absolute value of the second term in inequation 9 is much larger than that in eq 10, so that the latter can be ignored in our estimation, which also means that the values of E_1, E_2, $E_{4.1}$, and $E_{4.2}$ have little effect on the threshold for excitability. Setting $f_{c_0} = 3.0$[22] gives $\ln\{\Theta[f_{c_0}, q_{c_0}]\} = -6.894$ in inequation 9. Then using the maximum and minimum values of T_c in inequation 9, respectively, we obtain 13 kJ/mol $\leqslant E_3 - E_5 \leqslant$ 46 kJ/mol. As $E_5 \approx$ 70 kJ/mol, 83 kJ/mol $\leqslant E_3 \leqslant$ 116 kJ/mol.

Figure 5 compares the theoretical predictions (eq 8) with our experimental observations at the onset of excitable waves in the control parameter plane of ($[H_2SO_4]$, temperature). Panels a, b, c, and d show when E_3 is taken as 83, 90, 100, and 116 kJ/mol, respectively. Since in our analysis we cannot get the formula of f as a function of temperature and $[H_2SO_4]$, we cannot nail the value of E_3. Instead, in Figure 5 we give the upper and lower boundaries of the theoretical prediction, which are calculated when the value of f_c is set to be $f_c = 4$ and $f_c = 1 + \sqrt{2}$, respectively. In our experiment, $1 + \sqrt{2} \leqslant f_c \leqslant 4$ within the range of 286 K $\leqslant T \leqslant$ 310 K, thus $E_3 = 83$ kJ/mol (Figure 5a) and $E_3 = 116$ kJ/mol (Figure 5d) can be ruled out, because the experimental data exceeds the upper or lower boundary when we consider the exact value of $\ln\{\Theta[f_c, q_c(T_c)]\}$. After excluding several values in this manner, the value of E_3 should be in the range of 83 kJ/mol $< E_3 <$ 113 kJ/mol, which is consistent with our analysis presented above. If we investigate $[H_2SO_4]_c$ in a wider range of temperature, a narrower range of E_3 can be obtained. The thick line of Figure 5c is a theoretical prediction of the onset when the value of f_c is fixed at $f_{c_0}(3.0)$. One observes that the fitted line agrees well with the experimental data. This result hints that, if the effect of temperature and $[H_2SO_4]$ on f can be canceled at the onset, the value of E_3 should be 100 kJ/mol so that the ϵ in the Oregonator model would be fixed at the onset. This conclusion must be tested by other experiments.

Temperature Effect on the Excitable Wave Speeds

Because it is difficult to obtain the exact wave speed, we did not select it to estimate the activation energies, but rather just regarded it as a reference. The experimental results are represented as solid circles in Figure 6. We notice that, although the apparent shapes of these target waves are similar, their dynamics behaviors are different because of different temperatures.

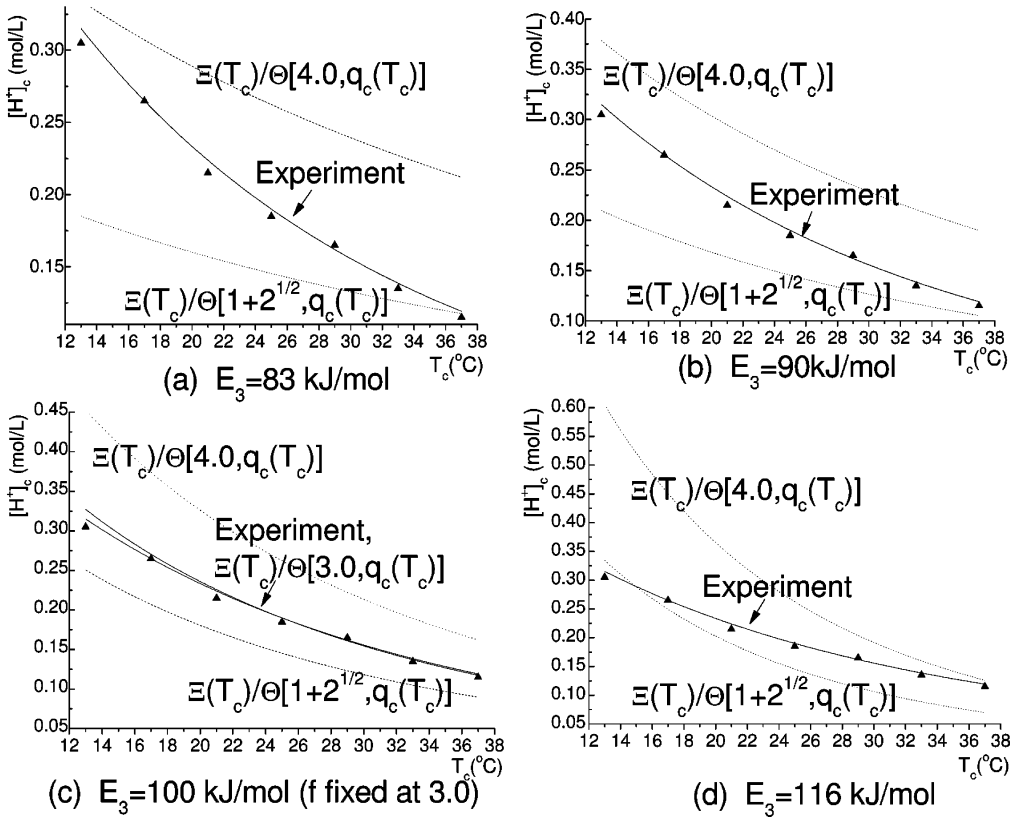

Figure 5. The calculated upper and lower limits of $[H]_c$ compared with the experimental results.

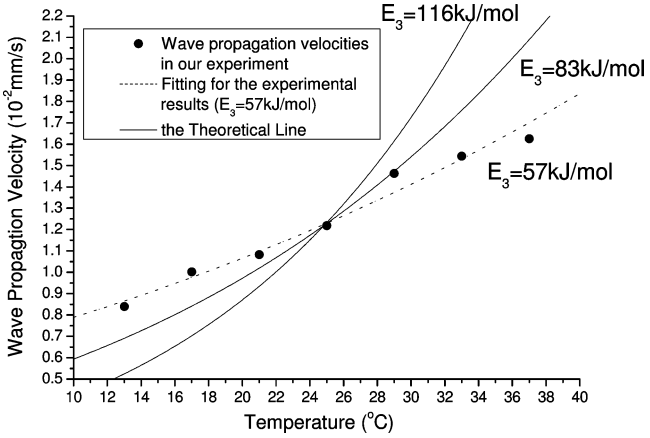

Figure 6. The excitable wave propagation velocity when $[H_2SO_4] \approx [H_2SO_4]_c$ at each temperature (T_c)

In the Oregonator model, the propagation velocity of an isolated excitable wave can be calculated by

$$\text{Velocity} = c(f,q,\upsilon_0)\sqrt{k_3[\text{H}][\text{A}]D_u} \qquad (11)$$

where $D_u = D_{u_0} \exp(-E_a/RT_c)$ (approximately, we use the value of E_a for water: $E_a \approx 15$ kJ/mol). When $[H_2SO_4] \approx [H_2SO_4]_c$, the wave period is long, so that we consider $c(f,q,\upsilon_0) \approx c[f_c,q_c,\upsilon_s(f_c,q_c)]$. Because $c\{f_c,q_c(T_c),\upsilon_s[f_c,q_c(T_c)]\}$ changes little under different temperatures as long as $1 + \sqrt{2} \leqslant f_c \leqslant 4$, we have the following approximation:

$$\text{Velocity} \approx c_0 \cdot e^{-[(E_3+\sigma+E_a)/2R][(1/T_c)-(1/T_{c0})]} \qquad (12)$$

where c_0 is the velocity of the wave front on $T_c = T_{c_0}$ and $[H]_c = [H]_{c_0}$. Taking $c_0 = 1.22 \times 10^{-2}$ mm/s when $T_0 = 298$ K, the theoretical line can be calculated. Figure 6 shows that the experimental observation on the wave speed as a function of T has the same trend as our expectation, but quantitative difference exists. We suggest that this discrepancy is mainly due to two factors. First, as temperature increases, the wave period decreases. As a result, the "wave back" does not have enough time to settle down, thus υ_0 does not really approach υ_s. Consequently, the measured wave propagation speed becomes smaller than that predicted in eq 12. Second, it has been reported that the wave period predicted by the Oregonator has a much weaker dependence on the hydrogen ion than that observed in experiments,[29,30] so that it predicts a much weaker dependence of the excitable wave speed on [H]. In other words, eq 11 may not quantitatively represent the velocity of the wave front, especially when we consider the effect of [H]. This also contributes to the discrepancy in Figure 6.

Discussion

The estimation of E_3 mentioned above results from the most possible values of q_{c_0} and f_{c_0}: $q_{c_0} = 0.0002$ and $f_{c_0} = 3.0$. Table 2 shows the results when q_{c_0} and f_{c_0} are selected as other possible values,[1,22] in which the maximum E_3 is 113 kJ/mol and the minimum E_3 is 80 kJ/mol. That means the more conservative estimation of E_3 is 80 kJ/mol $< E_3 <$ 113 kJ/mol.

In this paper, we estimated the activation energy E_3 without studying the details of the reaction processes of the BZ reaction, but rather through its global dynamics behaviors. Similarly, it is convenient to check the activation energies through the amplitude of oscillations or dynamics behaviors on different temperatures. For instance, as for the Oregonator, the dimensionless variable $u = (2k_4/k_3[\text{H}][\text{A}])[HBrO_2]$. When temperature changes, $u_{\min}$ and $u_{\max}$ change slightly, but k_4/k_3 changes a great deal. As a result, an Arrhenius dependence of the apparent amplitude of $[HBrO_2]$ on T possibly appears, so that $E_4 - E_3$ can be estimated. However, one of the potential difficulties is that some complex oscillations possibly emerge with increase in temperature. It has been reported that as temperature increases, a steady state will undergo transitions to chaos via complex oscillations.[23,24] This will complicate the estimation of $E_4 - E_3$.

TABLE 2: The Estimation of E_3 under Other Possible Values of q_{c_0} and f_{c_0} (Considering the Exact Value of $\ln\{\Theta[f_c, q_c(T_c)]\}$)

q_{c_0}			0.0002		0.0006	0.001	0.002
f_{c_0}		3.0	3.5	2.7	3.0	3.0	3.0
E_3	>	83	90	91	82	81	80
(kJ/mol)	<	113	107	105	107	103	94

Acknowledgment. We thank C. Qiao and C. X. Zhang for helpful discussion. This work is partially supported by the Chinese Natural Science Foundation and the Department of Science of Technology in China.

Note Added after ASAP Publication. This Article was published on Articles ASAP on January 24, 2007, with errors in the text above eq 4 and the equation for step ①, eq 5, and eq 7. The corrected version was reposted on January 31, 2007.

References and Notes

(1) Tyson, J. J. *Oscillations and Traveling Waves in Chemical Systems*; Field, R. J.; Burger, M., Eds.; Wiley-Interscience: New York, 1985.
(2) Scott, S. K. *Oscillations, Waves and Chaos in Chemical Kinetics*; Oxford University Press: New York, 1994.
(3) Nicolis, G; Prigogine, I. *Exploring Complexity*; W. H. Freeman and Company: New York, 1989.
(4) Kadar, S.; Wang, J.; Showalter, K. *Nature* **1998**, *391*, 770−772.
(5) Field, R. J.; Noyes, R. M. *J. Am. Chem. Soc.* **1974**, *96*, 2001−2006.
(6) Field, R. J.; Körös, E.; Noyes, R. M. *J. Am. Chem. Soc.* **1972**, *94*, 8649−8664.
(7) Kshirsagar, G.; Field, R. J. *J. Phys. Chem.* **1988**, *92*, 7074−7079.
(8) Ágreda, B. J. A.; Field, R. J. *J. Phys. Chem. A* **2006**, *110*, 7867−7873.
(9) Ruoff, P. *Physica D* **1995**, *84*, 204−211.
(10) Thompson, R. C. *J. Am. Chem. Soc.* **1971**, *93*, 7315−7315.
(11) Körös, E. *Nature* **1974**, *251*, 703−704.
(12) Blandamer, M. J.; Morris, S. H. *J. Chem. Soc., Faraday Trans. 1* **1975**, *71*, 2319−2330.
(13) Yoshikawa, K. *Bull. Chem. Soc. Jpn.* **1982**, *55*, 2042−2045.
(14) Abe, J.; Matsuda, K.; Taka, M.; Shirai, Y. *Chem. Phys. Lett.* **1995**, *245*, 281−286.
(15) Nagy, G.; Koros, E.; Oftedal, N.; Tjelflaat, K.; Puoff, P. *Chem. Phys. Lett.* **1996**, *250*, 255−260.
(16) Miyazaki, J.; Yoshioka, S.; Kinoshita, S. *Chem. Phys. Lett.* **2004**, *387*, 471−475.
(17) Karma, A. *Phys. Rev. Lett.* **1991**, *66*, 2274−2277.
(18) Ouyang, Q.; Swinney, H. L. *Chaos* **1991**, *1*, 411−420.
(19) Zykov, S. V.; Showalter, K. *Phys. Rev. Lett.* **2005**, *94*, 068302.
(20) Tyson, J. J.; Keener, J. P. *Physica D* **1987**, *29*, 215−222.
(21) Tyson, J. J.; Fife, P. C. *J. Chem. Phys.* **1980**, *73* (5), 2224−2237.
(22) Jahnke, W.; Skaggs, W. E.; Winfree, A. T. *J. Phys. Chem.* **1989**, *93*, 740−749.
(23) Masia, M.; Marchettini, N.; Zambrano, V.; Rustici, M. *Chem. Phys. Lett.* **2001**, *341*, 285−291.
(24) Stryzhak, P. E.; Didenko, O. Z. *Teor. Eksp. Khim.* **1995**, *31* (2), 69−75.
(25) Stryzhak, P. E.; Didenko, O. Z. *Teor. Eksp. Khim.* **1997**, *33* (3), 159−164.
(26) Belmonte, A. L.; Ouyang, Q.; Flesselles, J. M. *J. Phys. II (France)* **1997**, *7*, 1425−1468.
(27) Li, G.; Ouyang, Q.; Petrov, V.; Swinney, H. L. *Phys. Rev. Lett.* **1996**, *77*, 2105−2108.
(28) Ouyang, Q.; Flesselles, J. M. *Nature* **1996**, *379*, 143−146.
(29) Smoes, M. L. *J. Chem. Phys.* **1979**, *71*, 4669−4679.
(30) Edelson, D. *Int. J. Chem. Kinet.* **1981**, *13* (11), 1175−1189.